Canadian Science Publishing | Canadian Geotechnical Journal

Generalized effective stress concept for saturated active clays

Journal:	*Canadian Geotechnical Journal*
Manuscript ID	cgj-2020-0390.R1
Manuscript Type:	Article
Date Submitted by the Author:	20-Oct-2020
Complete List of Authors:	Tuttolomondo, Angelica; Ecole Polytechnique Federale de Lausanne, Soil Mechanics Laboratory Ferrari, Alessio; Ecole Polytechnique Federale de Lausanne, Soil Mechanics Laboratory Laloui, Lyesse; Swiss Federal Institute of Technology, EPFL
Keyword:	osmotic suction, Terzaghi, effective stress, active clays, saturated soils
Is the invited manuscript for consideration in a Special Issue? :	Not applicable (regular submission)

Generalized effective stress concept for saturated active clays

Angelica Tuttolomondo[1*], Alessio Ferrari[1,2],

and Lyesse Laloui[1]

[1]Ecole Polytechnique Fédérale de Lausanne (EPFL), School of Architecture, Civil and Environmental Engineering (ENAC), Laboratory for Soil Mechanics (LMS), EPFL-ENAC-LMS, Station 18, CH-1015 Lausanne, Switzerland

[2]Università degli Studi di Palermo, Dipartimento di Ingegneria Civile, Ambientale, Aerospaziale, dei Materiali (DICAM), Palermo, Italy

Emails of all the authors:

angelica.tuttolomondo@epfl.ch, alessio.ferrari@epfl.ch, lyesse.laloui@epfl.ch

*Corresponding author: Angelica Tuttolomondo

E-mail: angelica.tuttolomondo@epfl.ch

Phone: +41779905741 - +41 21 693 23 33

Abstract

Experimental evidence shows that changes in pore water chemistry can significantly affect the mechanical behavior of saturated active clays. Despite this evidence, how the chemical composition of the pore water can be considered in effective stress definition is questionable. This paper develops the concept of generalized effective stress for active clays. To this end, physicochemical studies on water–clay mineral interactions are used to clearly define the different types of ions and water present in an active clay. In particular, the presence of both movable and non-movable ions within the liquid water is highlighted. Taking this into account, thermodynamic and geochemistry principles are applied to the representative elementary volume scale for determining the pore water pressure and redefine the effective stress accordingly. The theoretical development results in the dependence of the effective stress on the pore water chemistry through the effective solute suction variable. Equations for the determination of this chemical variable are developed. The implications of the use of the proposed effective stress concept are investigated using experimental results taken from the literature. The results show advantages both in the interpretation of shear strength and volumetric data, and all support the theoretical explanation underlying the proposed concept.

Keywords: osmotic suction, Terzaghi, effective stress, active clays, saturated soils

Introduction

Active clays (Skempton 1953) are frequently involved in scenarios in which changes in the chemical composition of pore water can occur within the time scale of engineering interest. Such changes can subsequently modify the activity of the involved clays. For instance, such geomaterials can constitute a thin layer within a geosynthetic clay liner (GCL) (Bouazza et al. 2007; Seiphoori et al. 2016), represent one or more geological barriers in nuclear waste disposals (Ferrari et al. 2014; Mokni et al. 2014), be part of slopes where pore water chemical changes occur (Di Maio et al. 2016), and be involved in excavations for civil or oil purposes (van Oort 2003). Over the past decade, an increasing number of researchers have investigated the mechanical impact of the change in concentration of one or more substances (organic or inorganic, with possible pH variations) within the pore water. The main findings for an increase in salt concentrations in saturated clays can be summarised as follows: (i) reduction in liquid limit (Anson and Hawkins 1998); (ii) reduction in compression and swelling indices (Dutta and Mishra 2016; Yukselen-Aksoy et al. 2008); (iii) compression strain (Barbour and Fredlund 1989; Barbour and Yang 1993; Mokni et al. 2014; Witteveen et al. 2013); (iv) reversible strain under low external stress when the concentration changes involve exchangeable ions (Di Maio 1996); (v) change in shear strength (Calvello et al. 2005; Di Maio 2004); (vi) decrease in yield stress (Witteveen et al. 2013). The main factors affecting the magnitude of the evidence mentioned above are external load (Di Maio 1996), chemical history (Chen et al. 2017; Ye et al. 2017), range in which the concentration change occurs (Calvello et al. 2005), and smectite content (Di Maio and Fenelli 1994).

If a single-mechanical stress variable approach is chosen (i.e., the effective stress is the only mechanical stress variable governing the strain of the soil skeleton) and the mechanical effects induced by chemical changes are to be considered, it is clear from the above-mentioned experimental studies that the Terzaghi's effective stress cannot be regarded as suitable for saturated active clays.

A considerable number of effective stress definitions, potentially eligible for a single-mechanical stress variable, have been developed for clays. However, the complexity of determining the magnitude of attraction and repulsive interparticle stresses, for instance, has limited the adoption of the models derived at the particle scale (Lambe and Whitman 1969; Lambe 1960; Mitchell and Soga 2005; Sridharan and Rao 1973). These models are generally used for qualitative evaluations or back computations of the electrochemical terms under certain specific conditions (Lambe and Whitman 1969; Lambe 1960; Mitchell and Soga 2005; Sridharan and Rao 1973). A review of these models up to 1992, and a theoretical justification for their applicability, were provided by Hueckel (1992). A swelling pressure term as a function of the salt concentration of the bulk solution, as well as of microstructural parameters, is introduced within an effective stress formulation for saturated bentonites (Dominijanni and Manassero 2012a; Dominijanni et al. 2013). Under the hypothesis of parallel saturated aggregate layers, Xu et al. (2014) defined 'osmotic stress' as a function of the osmotic suction of the pore water and surface fractal dimension of the clay aggregates. Di Maio and Scaringi (2016) report that such a model is not successful for

the unified interpretation of residual shear strength at various salt concentrations.

A more general expression of effective stress is developed by Wei (2014). The theoretical derivation approach implicitly considers all the cations dissociated from the surface of the clay particles as part of the pore liquid water and associates to the pore liquid water a chemical potential component related to adsorptive forces. As a result, the different structural characteristics of water near clay particles are not considered. Furthermore, a significant drawback of all existing modeling approaches is that the chemical variable(s) being introduced within the definition of the effective stress are not always analytically defined. Therefore, its (their) value(s), along with a generalized stress path, is often unknown.

In this paper, experimental studies on the properties of water and ions near charged surfaces are first presented. In the light of them, a clear distinction between the types of ions and water existing in an active clay is given. A thermodynamic approach, coupled with geochemistry principles, is adopted for the determination of the pore water pressure at the representative elementary volume (REV) scale. The obtained expression of pore water pressure comprises a variable named effective solute suction, which depends, among other factors, on the pore water chemical composition. The Terzaghi's effective stress is then redefined accordingly. The proposed generalized effective stress concept includes both the definition of the effective stress variable and the analytical formulation needed for determining the effective solute suction stress variable. Shear strength and volumetric behavior are analyzed using the proposed concept. The results are discussed, and concluding remarks which can be drawn from

this work are presented.

Generalized effective stress concept for saturated active clays

With reference to active clays, this section introduces the (a) definition of the types of water and ions existing in active clays, (b) analytical expression of the pore water pressure under saturated conditions, (c) generalized effective stress concept for saturated media, and (d) mathematical formulations for the effective solute suction stress variable, the latter is needed for computing the pore water pressure and effective stress.

Water and ions definitions in active clays

Clay particles consist of a collection of 2-layer or 3-layer platelets with a crystalline structure. On the external surfaces of these particles, cations ensure the electroneutrality. The presence of polar water molecules in clays implies a partial (or complete) dissociation of these cations (Beek et al. 1978), which leads to a deficiency of positive charge on the external surfaces. Whereas, hydrogen ions can be adsorbed on the edges of the particles, depending on the pH of the solution (Beek et al. 1978).

The physical-chemical characteristics of water near the surface of a clay particle (hydrophilic/hydrophobic surface) (Saada et al. 1995; van Oss and Giese 1995) are still not well known (Chen et al. 2018). Experimental evidence indicates progressive changes in water structure (Asay and Kim 2005; Chen et al. 2018; Mante et al. 2014; Zhao et al. 2015). Laboratory experiments (Asay and Kim 2005; Cantrell and Ewing

2001; Cheng et al. 2001; Mante et al. 2014; Zhao et al. 2015) and molecular dynamics simulations (Odelius et al. 1997; Park and Sposito 2002) confirm the presence of water with ordered structure near minerals' surfaces. This ordered structure (due to water–mineral hydrogen bonding) involves up to four molecular water layers, with a maximum thickness of 1 nm (10 Å). Water density (Adapa and Malani 2018; Cheng et al. 2001; Mante et al. 2014; Park and Sposito 2002; Tournassat et al. 2009), viscosity (Mante et al. 2014), elastic properties (Mante et al. 2014), and diffusion coefficient typically vary within 1 nm from the mineral surface (Tournassat et al. 2009). These water properties remain constant beyond 1 nm from the surfaces.

Cations ensuring the electroneutrality of clay particles and dissociated from their surfaces may be at distances greater than 1 nm. Molecular dynamics simulations, as well as triple-layer and modified Gouy–Chapman models, show the possible presence of dissociated cations even when water density and diffusivity are equal to those of the bulk water (Tournassat et al. 2009). Terzaghi et al. (1996) report the presence of dissociated cations at a distance up to approximately 50 nm, depending on the pore size and chemical composition of the bulk water.

In light of the experimental evidence and to fully understand the theoretical treatment developed in the next subsection, the following terminology is proposed and adopted in this paper[1] (Fig. 1):

- *Solid water* is the water characterized by an ordered structure and located

[1] A complete list of definitions used in this paper is provided in the Supplementary material A.

within 1 nm from the surfaces of the clay minerals. It includes part or all of the cations necessary for balancing the negative charge on the minerals' surfaces.

- *Liquid water/pore water* refers to the water characterized by a disordered structure and whose properties no longer vary as the distance from the minerals' surfaces varies.
- *Diffuse layer* is the layer of water which includes cations that balance the negative charge on the external surfaces of clay minerals. It contains solid water and, depending on its thickness, may include liquid water.
- *Bulk water/free water* refers to the water located at a sufficient distance from clay particles such that it does not include any cations balancing the negative charge on the minerals' surfaces.
- *Movable ion* is a solute ion which belongs to the bulk water.
- *Non-movable ion* is a solute ion which is partially (or completely) dissociated from the particle surfaces; this ion cannot leave the diffuse layer. It can be exchanged with other ions of the bulk water, provided the negative charge of the external surfaces remains balanced within the diffuse layer.

Worthily, liquid water can contain both movable and non-movable ions (Fig. 1). Negative charge within the diffuse layer and pH-dependent charge on the edges of the particles are not considered because of a negligible entity compared to the positive one on the external surfaces (the number of anions in the diffuse layers and on the edges can be, for each of the two sites, in the range of 1-5% of the total number of cations exchangeable per unit mass of soil (*CEC*) (Beek et al. 1978)).

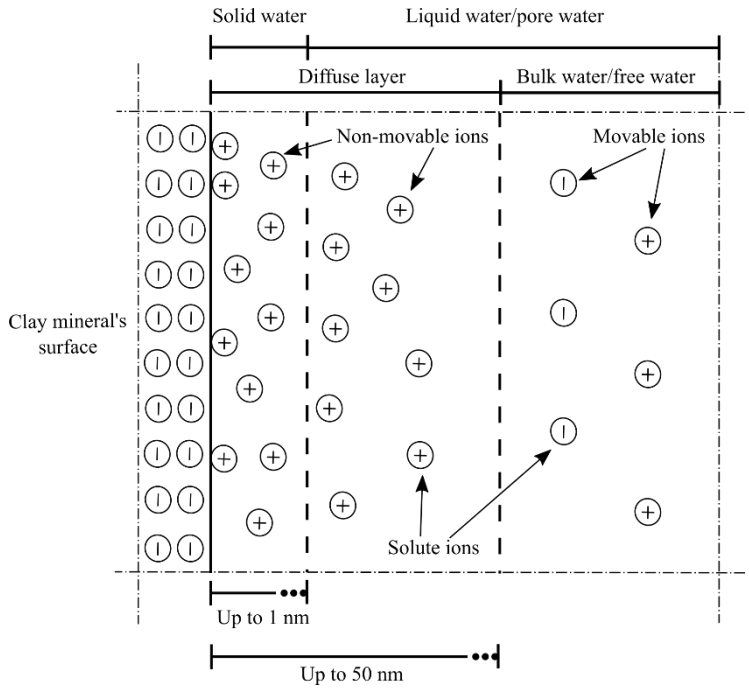

Fig. 1. Water and ions definitions in active clays.

Pore water pressure in saturated active clays

In this subsection, the pressure of pore water in saturated active clays is determined by adopting a thermodynamic approach and considering the presence of both movable and non-movable ions in the liquid water.

To this end, the theoretical physical model depicted in Fig. 2 is considered. The system includes the following: (a) the REV (centimeter scale) of an active clay in a closed container (System A); (b) a closed container connected to System A by a membrane permeable to both movable ions and water molecules (System B); (c) a closed container of pure water connected to System B by a membrane permeable only to water molecules (System C); (d) a piezometer connected to System A through a membrane permeable to both movable ions and water molecules (System P) (a positive pore water pressure is assumed); (e) a differential manometer connected to Systems B and C

(System M). All these components are in thermodynamic equilibrium.

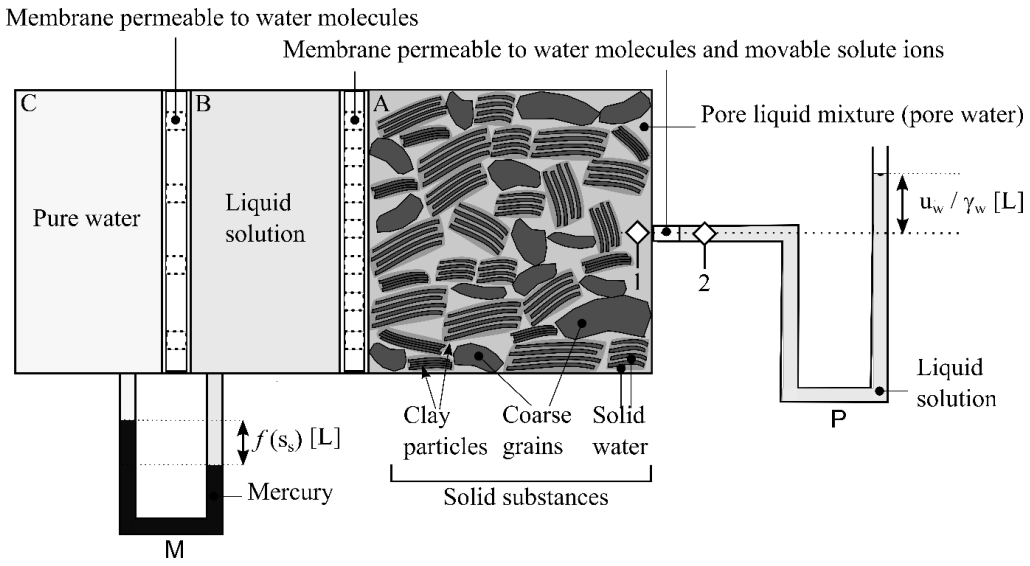

Fig. 2. Theoretical physical model adopted for the determination of the pore water pressure of a saturated active clay (size of the solid components is not at the scale).

The REV of the active clay (System A) is considered as a thermodynamic system consisting of (i) a non-homogenous mixture of solid substances (coarse grain, clay particles, and solid water); and (ii) an incompressible pore liquid mixture (the pore water), characterized by a volatile solvent (water) and different non-volatile solute ions (non-movable and movable ions). It is pointed out that, for the correct definition of the pore water pressure and as conventionally done in soil mechanics (Lambe and Whitman 1969), the substances within the REV are differentiated according to their state of aggregation.

Under these conditions, a thermodynamic approach is adopted. In particular, the principle of thermodynamic equilibrium relative to a generic constituent of a mixture

(Atkins and de Paula 2006; Castellan 1983) is applied to water at points 1 and 2 (at the same elevation) of Systems A and P, respectively (Fig. 2).

Considering the general expression of the chemical potential for an uncharged constituent of a real liquid mixture (Castellan 1983), the chemical potentials of water at points 1 and 2 (Fig. 2), at temperature T and reference pressure u^0, are

$$\mu_{w,1}[T,u_{w,1},a_{w,1}] = \mu_w^0[T,u^0] + \overline{V_w^0}(u_{w,1}-u^0) + RT\ln a_{w,1},$$
$$\mu_{w,2}[T,u_{w,2},a_{w,2}] = \mu_w^0[T,u^0] + \overline{V_w^0}(u_{w,2}-u^0) + RT\ln a_{w,2}, \quad (1)$$

where μ_w^0 is the chemical potential of pure water; $\overline{V}_w^0$ is the molar volume of pure water; R is the gas constant; $u_{w,1}$ and $u_{w,2}$ are water pressures at points 1 and 2, respectively; $a_{w,1}$ and $a_{w,2}$ are water activities at points 1 and 2, respectively. Imposing the equality of the chemical potentials (eq. (1)) gives

$$u_{w,1} = u_{w,2} + \frac{RT}{\overline{V_w^0}}\ln\frac{a_{w,2}}{a_{w,1}}. \quad (2)$$

The activity of a volatile constituent, such as water, is defined as the ratio between the vapor pressure above the liquid mixture (water and solutes) and the vapor pressure of the pure liquid (water) (Castellan 1983); therefore, it is independent of the point under examination both in System A and System P. Equation (2) becomes

$$u_{w,1} = u_{w,2} + \frac{RT}{\overline{V_w^0}}\ln\frac{a_w}{a_{pw}}, \quad (3)$$

where a_w is the activity of the water within System P; a_{pw} is the activity of the pore water. The latter depends on the presence of both movable and non-movable ions (Fig.1).

Neglecting the differences in the geodetic elevations of the points within the systems (both the REV and System P), the pore water pressure can be expressed as

$$u_{pw} = u_{w,1} = u_w + \frac{RT}{V_w^0} \ln \frac{a_w}{a_{pw}}, \tag{4}$$

where u_w is the water pressure measured (or imposed) externally.

Equation (4) can be rewritten by recognizing in it some quantities already known in the literature and hereinafter recalled.

In particular, moving from the definition of the solute (osmotic) potential in Romero (1999), the solute suction for the water in System P can be expressed as

$$s_s = -\frac{RT}{V_w^0} \ln \frac{u_{v,w}}{u_v^0}, \tag{5}$$

where $u_{v,w}$ is the vapor pressure of the water in System P; u_v^0 is the vapor pressure of the pure liquid; $u_{v,w}/u_v^0$ is the activity of the water in System P (a_w). The minus sign in eq. (5) accounts for the fact that solute suction assumes positive values when the solute potential is negative. The term s_s can be computed from Fig. 2 using systems B, C, and M (see Appendix A). Since the membrane between System A and System P is permeable to water molecules and movable ions and all systems are at equilibrium, s_s is also the solute suction of the bulk water.

Similarly, it is possible to obtain the solute suction of the pore water as

$$s_{s,pw} = -\frac{RT}{V_w^0} \ln \frac{u_{v,pw}}{u_v^0}, \tag{6}$$

where $u_{v,pw}$ is the vapor pressure of the pore water; $u_{v,pw}/u_v^0$ is the activity of the pore water (a_{pw}).

Equations (5) and (6) enable writing eq. (4) as follows

$$u_{pw} = u_w + s_{s,pw} - s_s. \quad (7)$$

The difference between the two solute suction terms in eq. (7) is defined in this study as *effective solute suction*:

$$s_{s,e} = s_{s,pw} - s_s. \quad (8)$$

At a given temperature, $s_{s,pw}$ is related to the presence of movable and non-movable ions; s_s is linked only to movable ions. Therefore, $s_{s,e}$ (eq. (8)) has a higher positive value as the number of non-movable ions belonging to the liquid water increases; while $s_{s,e} = 0$ when these ions are not present. The methodology for the computation of $s_{s,e}$ is discussed in a separate subsection later in the paper.

Equation (7) becomes

$$u_{pw} = u_w + s_{s,e}. \quad (9)$$

Effective stress concept

The developed formula of u_{pw} (eq. (9)) explicitly accounts for the chemical interaction between clay particles and water molecules; therefore, it is considered as the more convenient expression for defining the effective stress of saturated active clays. Replacing eq. (9) in the Terzaghi's effective stress, allows expressing the *generalized effective stress for saturated active clays* as follows

$$\sigma'_{ij} = \sigma_{ij} - (u_w + s_{s,e})\delta_{ij} \quad (10)$$

where σ_{ij} is the total stress tensor, $u_w\delta_{ij}$ is the measured (or externally imposed) water pressure tensor, and $s_{s,e}\delta_{ij} = (s_{s,pw} - s_s)\delta_{ij}$ is the effective solute suction stress tensor. In the case of non-active clays, or any other geomaterial where the interaction between solid particles and water molecules is not significant, any non-movable ions belong to the pore water, $s_{s,e} = 0$ and the Terzaghi's effective stress is restored.

The developed effective stress (eq. (10)) allows considering, concomitantly, the mechanical effects related to total stress, water pressure, and pore water chemical composition.

For the generalized effective stress (eq. 10) to be determined, the $s_{s,e}$ at a generic state of the active clay, as well as its variation along with a generalized saturated stress path, is required. A suitable formulation for computing $s_{s,e}$ is provided in the following subsection.

The definition of the effective stress σ'_{ij} (eq. (10)), as well as of the additional chemical variable needed for its computation (i.e., $s_{s,e}$), if combined with a suitable stress-strain constitutive model, form the *concept of generalized effective stress for active clays*.

Effective solute suction

The effective solute suction ($s_{s,e}$) is the difference between the solute suction of the pore water ($s_{s,pw}$) and the solute suction of the bulk water (i.e., of the liquid solution in System P) (s_s) (eq. (8)). One of the following options can be adopted for computing s_s at a given temperature:

(1) use of a dew-point chilled-mirror psychrometer (Decagon, WP4C) (Cardoso et al. 2007; Decagon 2010; Witteveen et al. 2013): the bulk water (or a solution with the same chemical composition of the bulk water; in this case, prior knowledge of the chemical composition of the bulk water is required) is inserted inside a sealed chamber and the vapor pressure in equilibrium with the tested solution ($u_{v,w}$ in eq. (5)) is determined; typically, the instrument provides the water potential, the opposite of which is the suction of interest.

(2) Use of tabulated values (Fredlund and Rahardjo 1993), or use of empirical formulas correlating the concentration of salts in the liquid solution with the solute suction of water. For NaCl solutions, an empirical expression based on different data existing in the literature is provided later in this paper. Prior knowledge of the chemical composition of the bulk water is needed.

(3) Solving equation (5) by assuming the equality between activity and mole fraction of water in bulk water (ideal liquid). The mole fraction of water can be estimated once the concentrations of the ions in the bulk water are determined (bulk water can be extracted by means of a fluid squeezer (Fredlund and Rahardjo 1993); ions concentration can be determined, for instance, through ion chromatography).

The determination of $s_{s,pw}$ requires the application of electrochemical and electroneutrality principles for the contextual determination of the pore water chemical composition.

This subsection presents the main equations for computing $s_{s,e}$ when the pore water and the bulk water are ideal. To this end, all the systems of Fig. 2 are considered to be in thermodynamic equilibrium and electroneutral.

Considering the general expression for the electrochemical potential of a charged constituent (positive or negative) of an ideal liquid mixture (Atkins and de Paula 2006; Castellan 1983), the thermodynamic equilibrium between point 1 and 2 (Fig. 2) is established when the following relations are valid:

$$\mu_{+,1}[T,u_{w,1},x_{+,1},\gamma_{+,1}] = \mu_{+,2}[T,u_{w,2},x_{+,2},\gamma_{+,2}],$$
$$\mu_{-,1}[T,u_{w,1},x_{-,1},\gamma_{-,1}] = \mu_{-,2}[T,u_{w,2},x_{-,2},\gamma_{-,2}], \quad (11)$$

where $\mu_{+,1}$ and $\mu_{+,2}$ are the electrochemical potentials of a certain positive ion (the same in the two liquids) situated at points 1 and 2; $\mu_{-,1}$ and $\mu_{-,2}$ are the electrochemical potentials of a certain negative ion (the same in the two liquids) situated at points 1 and 2; $x_{+,1}$, $x_{-,1}$, $x_{+,2}$ and $x_{-,2}$ are the mole fractions of the considered ions in the two systems; $\gamma_{+,1}$, $\gamma_{+,2}$, $\gamma_{-,1}$, and $\gamma_{-,2}$ are the activity coefficients of the considered ions in the two systems. Under the hypothesis of ideal solutes (or real solutes having the same activity coefficients) of equal valence numbers, a relation between the mole fractions of the considered two types of solute ions (a positive and a negative one) can be written (see Appendix B)

$$x_{+,1}x_{-,1} = x_{+,2}x_{-,2}. \quad (12)$$

Within the logic of the representative elementary volume in the context of continuum mechanics, the effects of punctual variation of the involved quantities are neglected in both systems. Therefore

$$x_{+,pw}x_{-,pw} = x_{+}x_{-} \quad (13)$$

where $x_{+,pw}$, $x_{-,pw}$, x_{+}, and x_{-} are the mole fractions of the considered ions in the pore water and in System P. For pore water, the values are intended to be calculated as the average values for the entire REV.

Adopting a similar approach to that of Wei (2014), the electroneutrality condition (number of moles of positive charge equal to those of negative charge, per unit of mass of solution) of System P can be expressed as

$$\frac{\sum_k \nu_{+k} x_{+k}}{x_w M_w} = \frac{\sum_l \nu_{-l} x_{-l}}{x_w M_w} = \frac{c_0}{\rho_w}, \tag{14}$$

where ν_{+k}, ν_{-l} and x_{+k}, x_{-l} are the valence numbers and the mole fractions of the k-type positive ions and l-type negative ions, respectively; ρ_w, M_w and x_w are, respectively, the density, molar mass, and mole fraction of the water in System P; c_0 is the number of moles of charge per unit volume of the solution in System P.

The negative charge in System A includes the movable negative ions of the bulk water and the charge on the outer surface of the clay particles (Fig. 1). The number of moles of negative charge on the outer surface of the clay minerals, per unit volume of clay, is the density of fixed charge (c_{fix}) (Wei 2014); c_{fix} can be related to the Cation Exchange Capacity (*CEC*) of the clay:

$$c_{fix} = CEC 10^{-2} \rho_d, \tag{15}$$

where *CEC* is expressed in cmol/kg (or meq/100 g); and ρ_d is the dry density expressed in kg/m^3.

The negative charge, per unit volume of clay, balanced by the non-movable ions of the pore water, is introduced in this work and called *effective density of fixed charge* ($c_{fix,e}$); $c_{fix,e}$ can be computed as

$$c_{fix,e} = \delta c_{fix}, \tag{16}$$

where δ is a *reduction factor*, with $0 \leq \delta < 1$.

The positive charge in System A consists of the movable positive ions of the bulk water, non-movable positive ions of the solid water, and the non-movable positive ions of the pore water (Fig. 1).

The balance of charge between the ions in the solid water and the corresponding negative charge on clay particles is not of interest to this discussion. Therefore, the condition of electroneutrality for System A is written as

$$\frac{\sum_i \nu_{+i,pw} x_{+i,pw}}{x_{pw} M_{pw}} = \frac{\sum_j \nu_{-j,pw} x_{-j,pw}}{x_{pw} M_{pw}} + \frac{c_{fix,e}}{S_r n \rho_{pw}}, \tag{17}$$

where $\nu_{+i,pw}$, $\nu_{-j,pw}$ and $x_{+i,pw}$, $x_{-j,pw}$ are the valence numbers and mole fractions, respectively, of the *i*-type positive ions and *j*-type negative ions present in the pore water; ρ_{pw}, M_{pw} and x_{pw} are, respectively, the density, molar mass, and mole fraction of the pore water; n is the porosity and S_r is the degree of saturation, the latter is equal to one for a saturated active clay.

Electrochemical potential and electroneutrality equations (eqs. (13), (14), and (17)) can be used to compute $s_{s,e}$. In the case of ideal liquid, the ratio of the vapor pressure

above a liquid to the vapor pressure of the pure water is equal to the mole fraction of the water in the considered liquid (Raoult's law). It follows that

$$x_w = \frac{u_{v,w}}{u_v^0}, \qquad x_{pw} = \frac{u_{v,pw}}{u_v^0}. \tag{18}$$

If the mole fractions are used for computing a physical-chemical property dependent on the number of particles (like the vapor pressure, in this case), the ion concentrations should be used instead of the analytical ones (Silvestroni 1968).

For the case of one positive and one negative monovalent ion in the two systems, the mole fractions of the water are

$$x_w = 1 - x_+ - x_-, \qquad x_{pw} = 1 - x_{+,pw} - x_{-,pw}. \tag{19}$$

Because there is only one type of positive ion and only one type of negative ion in the two liquids ($k = l = i = j = 1$) and the ions considered are monovalent ($\nu_{+k} = \nu_{-l} = \nu_{+i,pw} = \nu_{-j,pw} = 1$), the electroneutrality equations (eqs. (14) and (17)) for ideal liquids become

$$\frac{x_+}{M_w} = \frac{x_-}{M_w} = \frac{c_0}{\rho_w}, \tag{20}$$

$$\frac{x_{+,pw}}{M_{pw}} = \frac{x_{-,pw}}{M_{pw}} + \frac{c_{fix,e}}{S_r n \rho_{pw}}. \tag{21}$$

Once the chemical composition of the bulk water (i.e., c_0 in eq. (20)) and the other terms appearing in eqs. (20) and (21) are known, the mole fraction of positive and negative ions in the pore water can be computed by solving eqs. (13) and (21) for the unknowns $x_{+,pw}$ and $x_{-,pw}$. Mole fractions of water are computed by eq. (19). The solute suction of the water in System P and that of the pore water are calculated by equations (5), (6), and (18). $s_{s,e}$ is computed by eq. (8).

For low active clays, the diffuse layers near the clay particles only extend into the solid water and $\delta = 0$; the mole fractions of the solvent and solute ions are equal in the pore water and in the liquid of System P. Consequently, $s_s = s_{s,pw}$ (equations (5) and (6)) and $s_{s,e} = 0$ (eq. (8)). In this case, the Terzaghi's effective stress is restored (see eq. (10)).

Implications of the use of the generalized effective stress for saturated active clays

Shear strength behavior of saturated active clays

The generalized effective stress (eq. (10)), replaced in the Mohr-Coulomb shear strength criterion, allows expressing the shear strength of an active clay saturated with a pore water of a certain chemical composition as

$$\tau_f = c' + [\sigma_n - (u_w + s_{s,e})] \tan \varphi', \quad (22)$$

where $\boldsymbol{\tau_f}$ is the available shear strength on a given plane, $\boldsymbol{c'}$ and $\boldsymbol{\varphi'}$ are the effective shear strength parameters, $\boldsymbol{\sigma_n}$ is the total normal stress acting on the plane. The

difference $\boldsymbol{\sigma_n - u_w}$ is the Terzaghi's effective stress (Terzaghi 1936).

Shear strength tests performed on Ponza bentonite (clay fraction of 80%, specific gravity G_s=2.77; kaolinite and Na-smectite fractions of approximately 20% and 80%, respectively; $I_{p,DW} = 320\%$, $w_{l,DW} = 390\%$; Di Maio (1996); Di Maio et al. (2004)) are reported by Di Maio (1996). Specimens were prepared by mixing the powdered clay with NaCl solutions of various concentrations (distilled water DW, 0.2 M, 0.5 M, 1 M, and 6.1 M) at the corresponding liquid limits (estimated using the same solution used for testing). They were consolidated at approximately 400 kPa and sheared at various stresses in the conventional direct shear test apparatus until the residual state was reached. Shear strength against Terzaghi's effective stress is shown in Fig. 3a, together with the corresponding linear regression models (equations and determination coefficients). When all the data are considered, $R^2_{\tau(\sigma'_{n,Terzaghi})} = 0.74$.

To reinterpret the data according to eq. (22), $s_{s,e}$ for each experimental point is determined as the difference between the solute suction of the pore water and the solute suction of the water used for preparing and testing the specimens (eq. (8)). The former is computed collecting solute suction data for different NaCl concentrations (Lang 1967; Witteveen et al. 2013) and determining an interpolating polynomial function with $R^2 = 1.00$ (Fig. 4). To this end, the point (0,0) was added to the experimental series and the distinction between molarity and molality was neglected. Fig. 4 also provides the theoretical function (Raoult's law).

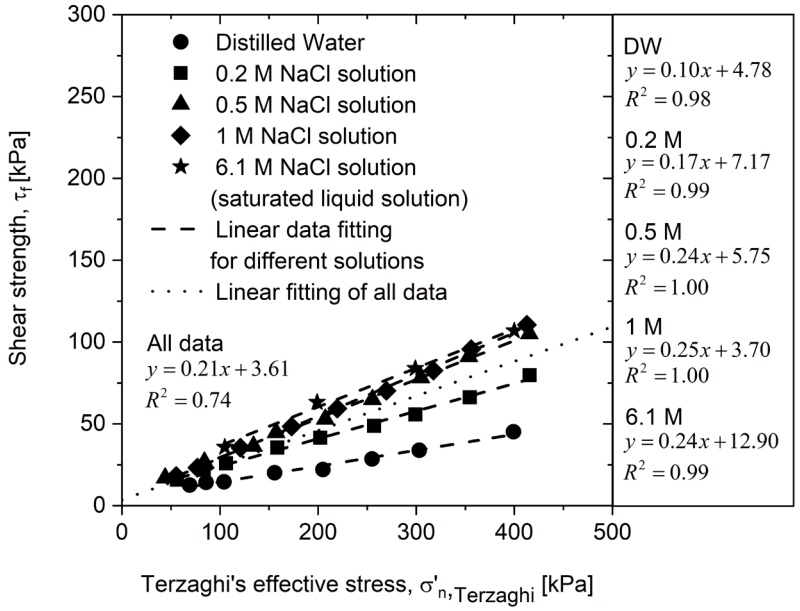

(a)

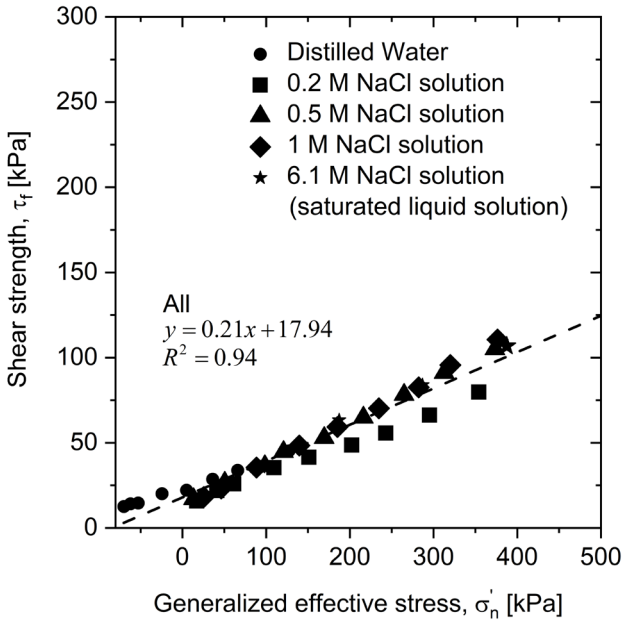

(b)

Fig. 3 Shear strength envelopes for various concentrations of NaCl according to the (a) Terzaghi's effective stress. (b) generalized effective stress. Linear regression models are provided in the figure. Experimental data reported by Di Maio (1996).

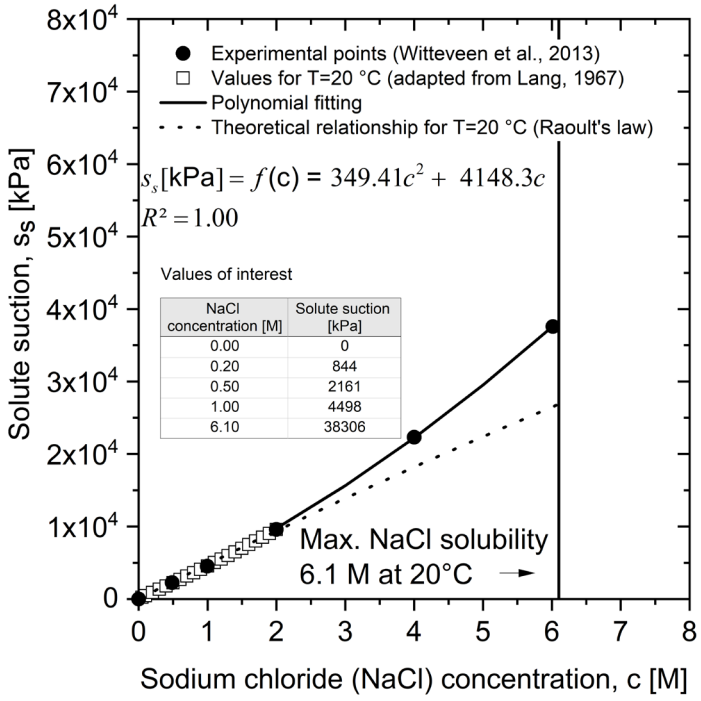

Fig. 4. Solute suction of NaCl solutions having various NaCl concentrations. The proposed polynomial function is provided in the figure, together with the values of interest. Experimental data from Witteveen et al. (2013) and (Lang 1967).

For computing $s_{s,pw}$, equations (13), (20) and (21) are solved. Void ratios are estimated using the oedometer curves of Ponza bentonite (Di Maio et al. 2004)[2]. The strain experienced by the specimens to reach failure is considered only for specimens with DW and has a negligible influence on $s_{s,e}$.

The *CEC* of a geomaterial with a negligible organic fraction can be estimated as:

[2] Details are provided in the Supplementary material B.

$$CEC = \sum_m CEC_m y_m, \tag{23}$$

where CEC_m and y_m are the cation exchange capacity and the fraction of the pure clay mineral m, respectively. For Ponza bentonite, based on data from the literature (Table 1), $CEC = 74$ cmol/kg (meq/100 g).

As a first approximation, δ is considered a material parameter. Its value, back predicted for ensuring the best coefficient of determination of the linear regression model associated with all the shear strength data, is equal to 0.15.

Fig. 3b shows the shear strength data interpreted adopting the generalized effective stress (eq. (22)). Table 2 lists the data. In this case $R^2_{\tau(\sigma'_n)} = 0.94$.

Volumetric change behavior of saturated active clays

Two different types of datasets are selected. The first dataset includes cyclic tests performed on saturated Ponza bentonite (clay fraction of 80%; kaolinite and Na-smectite fractions of approximately 20% and 80%, respectively; $w_p = 75.4\%$, $w_l = 390.2\%$, and $I_a = 3.9$) and Gela clay (clay fraction of 73%; smectite fraction of 30%; $w_p = 41.1\%$, $w_l = 148.6\%$, and $I_a = 1.5$) (Di Maio 1996; Di Maio and Fenelli 1997). Highly concentrated NaCl solution and DW were alternated (with continuous opportune renewals) in the oedometer cell at a constant stress of 40 kPa. The experimental data reveal a fully elastic strain.

The second dataset includes oedometer tests performed on saturated Ponza bentonite prepared with DW. Two different specimens are considered. The first one (Fig. 6a, left) was subjected to mechanical loading up to Terzaghi's effective stress of 1200 kPa. The specimen was next exposed to a 6.1 M NaCl solution and loaded up to 2500 kPa. After that, it was unloaded to 40 kPa, and the cell fluid was changed again to DW. The second specimen (Fig. 6b, left) was subjected to a similar chemo-mechanical path; however, DW was replaced by 6.1 M NaCl at a lower stress level.

For each experimental point, $s_{s,e}$ is computed following the same procedure described in the subsection 'Shear strength behavior of saturated active clays'. The solute suction of the liquid solutions used for preparing and testing the specimens are computed using the polynomial function provided in Fig. 4 (values summarized in the figure). For the computation of $s_{s,pw}$, the void ratios were either provided by the investigators, or they are estimated from the volumetric strain data by knowing the initial void ratio. Initial void ratios are calculated using the corresponding oedometer curves (Di Maio 1996; Di Maio and Fenelli 1997). The *CEC* values for Ponza bentonite and Gela clay are 74 cmol/kg and 27 cmol/kg, respectively (eq. (23), data from Table 1). A $\delta = 0.15$ is adopted for Ponza bentonite based on the shear strength analysis (subsection 'Shear strength behavior of saturated active clays). A $\delta = 0.11$ is adopted for Gela clay; this value is estimated assuming a linear variation of δ with respect to *CEC*. To this end, in addition to the data obtained for Ponza bentonite, it is also considered that, on average, for pure illite ($CEC_m = CEC = 20$ cmol/kg, Table 1), the fraction of cations in the layer nearest to the particle surface can be considered equal to 0.90 (Revil et al.

2013) (i.e., $\delta = 0.10$) (the linear relationship between δ and *CEC*, determined for the range of *CEC* of 20-74 $\mathrm{cmol/kg}$, is provided by the following expression: δ = 0.0009*CEC* + 0.0815).

Fig. 5 (first experimental dataset) reveals that elastic expansion (i.e., negative elastic strain) is associated with a decrease of the effective stress; while elastic compression (i.e., positive elastic strain) is related to an increase of the effective stress. This result agrees with the following relation

$$\dot{\varepsilon}_{ij}^{e} = C_{ijkl}^{e}\dot{\sigma}_{kl}^{'}, \tag{24}$$

where $\dot{\varepsilon}_{ij}^{e}$ is the rate of elastic strain of the soil skeleton, C_{ijkl}^{e} is the drained elastic compliance tensor, and $\dot{\sigma}_{kl}'$ is the extended generalized effective stress increment. Noteworthy, the adopted strategy of referring to experimentally observed elasticity is different from the most common methodology of assuming the occurrence of elastic strains (e.g. Mašín and Khalili 2016).

Fig. 6 (a and b) (second experimental dataset) shows the comparison of the interpretation of the oedometer curves according to Terzaghi's effective stress (left) and generalized effective stress (right). A unique continuous oedometer curve, regardless of the type of load (mechanical or chemical), is obtained if the proposed generalized stress is adopted.

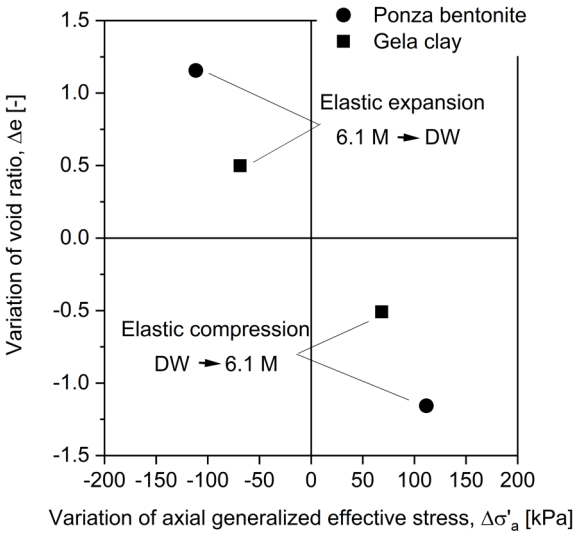

Fig. 5. Elastic cycles associated with pore water chemical changes. Experimental data reported by Di Maio (1996) (Ponza bentonite) and Di Maio and Fenelli (1997) (Gela clay).

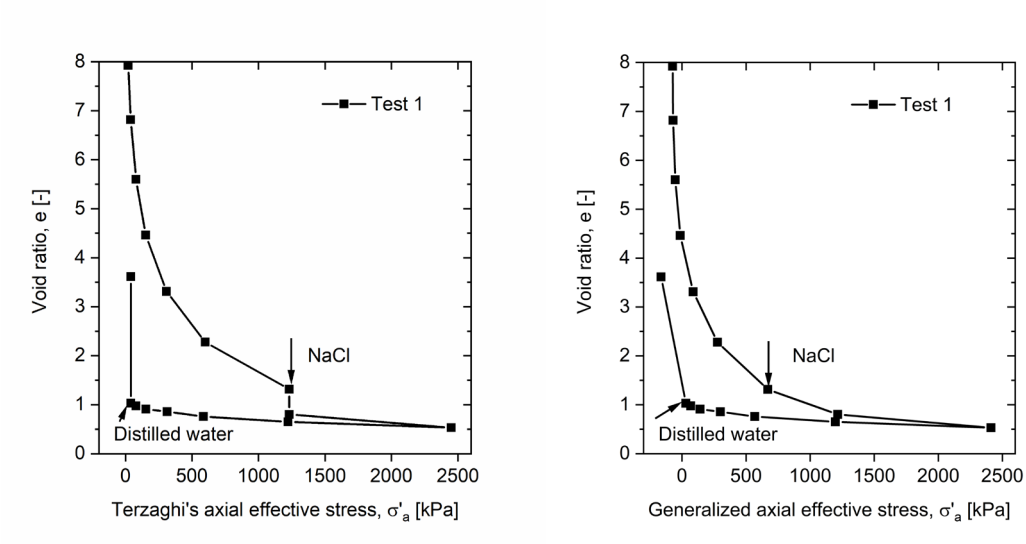

(a)

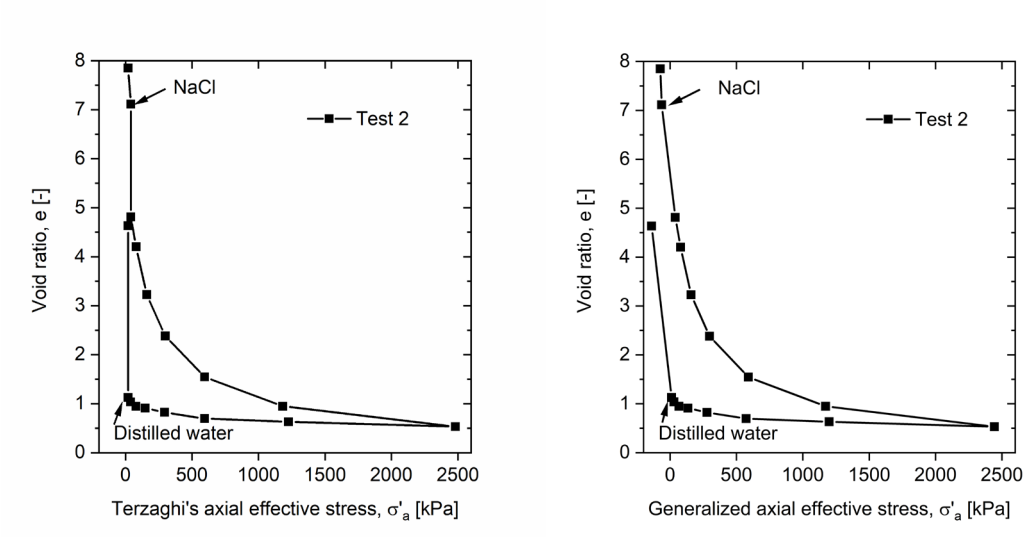

(b)

Fig. 6. Oedometer curves of Ponza bentonite subjected to chemo-mechanical paths according to two different interpretations ("NaCl" stands for 6.1 M NaCl solution): (left) Terzaghi's effective stress; (right) generalized effective stress. Experimental data reported by Di Maio (1996).

Discussion

Impact of solute concentration on generalized effective stress

Values of $s_{s,e}$ varying in the range 139–272 kPa are obtained for specimens of Ponza bentonite with DW; values of 11–12 kPa are estimated for 6.1 M NaCl solution (Table 2).

Fig. 7a shows the variation of $s_{s,e}$ at varying NaCl concentration for targeted Terzaghi's effective stresses (second-order polynomial function with $R^2 \geq 0.99$ was used for interpolating effective solute suction data against Terzaghi's effective stress). For a given Terzaghi's effective stress, $s_{s,e}$ decreases as the concentration of salts in the bulk water increases. The higher the concentration of salts in the bulk water, the lesser the impact of non-movable ions on the pore water chemistry. When $s_{s,e}$ tends to be zero, the pore water pressure becomes similar to the measured/imposed one (eq. 9),

and the generalized effective stress (eq. (10)) increases. In the limit case in which $s_{s,e} = 0$, the geomaterial - as long as the salt concentration does not decrease - can be modeled as a purely granular material, and the Terzaghi's effective stress is restored (eq. 10). An increase in salt concentration that causes the generalized effective stress to become equal to that of Terzaghi's one still has mechanical implications due to the induced variation in generalized effective stress.

For low concentrations, $s_{s,e}$ is high (Fig. 7a), and the generalized effective stress decreases (eq. 10).

A further reason that can lead to a reduction in $s_{s,e}$ when the salt concentration in the bulk water increases is the decrease in the diffusion propensity of non-movable ions. This reduction implies a lower presence of non-moveable ions in the bulk water, i.e., a smaller δ. For the sake of simplicity, this reduction was not considered in this study.

The increase in effective stress at increasing salts agrees well with the experimental studies reported in the literature (Di Maio 1996, 2004; Kenney 1967; Spagnoli et al. 2011).

The proposed interpretation agrees with the double-layer theory (Mitchell and Soga 2005): a higher concentration of salts within the bulk/free water implies a reduction in the thickness of the double layers and a lesser impact of the latter on the mechanical behavior of the geomaterial. The more the clay minerals have a positive charge deficit, the more significant this effect (Mitchell and Soga 2005).

Fig. 7a also shows that for a given concentration (especially if below 0.5 M), higher values of $s_{s,e}$ are obtained for higher Terzaghi's effective stresses, i.e., at lower void ratios (the pre-consolidation stress is equal to 400 kPa; the effective stresses lower than 400 kPa refer to states belonging to the unloading line). In fact, as the void ratio decreases, the non-movable ions belonging to the pore water are distributed over a smaller volume of water. Consequently, their concentration in the pore water is higher, so the difference between the chemical compositions of pore water and bulk water is more significant.

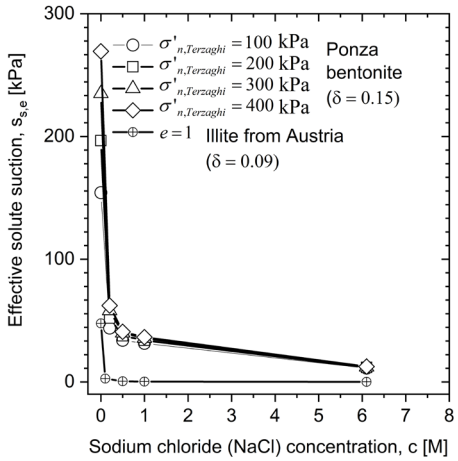

(a)

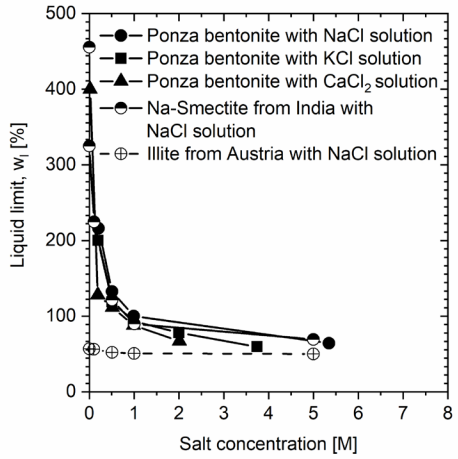

(b)

Fig. 7. (a) Effective solute suction for different NaCl concentrations; (b) liquid limit for various salt concentrations. Experimental data from Di Maio (1996) and Spagnoli et al. (2011).

The most significant range of solutes concentration

Fig. 7a shows, for Ponza bentonite and illite from Austria (*CEC*=8 cmol/kg, clay fraction of 48%, $e \simeq 1$) (Spagnoli et al. 2011), more significant variations of $s_{s,e}$ in the range of salt concentration of 0–0.5 M. It follows that changes of salt concentration in this range induces the highest changes in effective stress (eq. (10)). For the illite from Austria, a value of δ=0.09 is estimated assuming a linear variation of δ with respect to CEC (see "Volumetric change behavior of saturated active clays").

This result agrees with the experimental findings existing in the literature. For instance, 0–0.5 M is the range in which salt concentration changes imply significant variations in the liquid limit of Ponza bentonite (Di Maio 1996) and illite from Austria (Spagnoli et al. 2011) (Fig. 7b). For the latter, when the concentration is higher than 0.5 M, $s_{s,e} = 0$ (Fig. 7a) and a zero change in the liquid limit is consistently observed (Fig. 7b).

Liquid limit data for clay from India (Na-smectite, *CEC*=96 cmol/kg, clay fraction of 85%, Spagnoli et al. (2011)) (Fig. 7b) and other geomaterials (among others Di Maio and Scaringi 2016) support the same most significant range of solutes concentration.

Worthily, the same crucial oncentration range can also be detected by looking at the variations in the compression index (Di Maio et al. 2004), oedometer modulus (Witteveen et al. 2013), shear strength (Di Maio 2004; Di Maio et al. 2016), or swelling behavior (Manca et al. 2016).

δ reduction factor

Table 3 summarises the values of δ predicted or estimated in this paper. The magnitude of δ indicates the importance of considering the fraction of non-movable cations belonging to the pore water. This parameter is always less than one; it is zero if only movable ions are present in the liquid water (i.e., if the diffuse layer extends only within 1 nm from the particle surfaces). High δ implies a greater difference between the pore water pressure and the measured (or imposed), i.e., more significative values of $s_{s,e}$. For instance, the high smectite content in Ponza bentonite (almost 80%, Di Maio et al. 2004) (*CEC*=74 cmol/kg) leads to a significant presence of dissociable cations (Beek et al. 1978), a fraction of which belongs to the pore water ($\delta = 0.15$).

A parameter similar to δ is considered in other studies (Dominijanni and Manassero 2012a, 2012b; Goncalves et al. 2007; Revil et al. 2013). In particular, the complement to 1 of the so-called partition coefficient (or Stern fraction) is equal to δ when the Stern layer extends for 1 nm from the particle surfaces. For smectite, values of partition coefficients between 0.75 and 0.85 are predicted for salinity below 5 mmol/l and pH = 5.5 (Leroy and Revil 2009) ($\delta = 0.15$–0.25). For higher salinities, a maximum value of 1 is expected ($\delta = 0$). Partition coefficients in the range between 0.84 and 0.94 have been obtained in other studies (Leroy et al. (2007), Goncalves et al. (2007), Jougnot et al. (2009)) ($\delta = 0.06$–0.16).

Also, approximately 75% of cations are usually considered to reside within 1 nm from the particle surface (Mitchell and Soga 2005; Sposito 1989) ($\delta = 0.25$).

The δ, back predicted in this work for Ponza bentonite, agrees with the values reported in the literature for similar parameters; remarkably, the procedure in this study is based on a completely different procedure than the studies mentioned.

In addition to the possibility of estimating δ through the reinterpretation of shear strength results referred to specimens prepared at different salt concentrations, the linear relationship correlating δ to *CEC* provided in the subsection "Volumetric change behavior of saturated active clays" can be adopted as a first approximation.

Concluding remarks

This study presents the concept of generalized effective stress for saturated active clays. The adopted theoretical approach is based on principles of thermodynamics and geochemistry applied to the representative elementary volume scale. The physical-chemical interaction between clay minerals and water is explicitly considered by accounting for the presence of diffuse layers, and, in particular, of the so-called non-movable ions within the pore water. Under saturated conditions, taking into account the effect of these ions on the chemical composition of pore water proves to be suitable to justify the mechanical effects associated with variations in salt concentration.

The major implications in adopting the developed framework, verified by reinterpreting existing experimental results on saturated active clays, are the following:

(I) the failure envelope is unique irrespective of the chemical composition of the pore water. A unique set of saturated shear strength parameters can be defined;

(II) positive effective stress variations are observed in the case of elastic compression

strain due to salt concentration changes, negative effective stress variations are detected in the case of elastic swelling induced by salt concentration changes;

(III) the range of salt concentrations in which a change has more significative mechanical effects is implicitly considered;

(IV) the normal compression and unloading lines of chemo-mechanical paths are unique.

References

Adapa, S., and Malani, A. 2018. Role of hydration energy and co-ions association on monovalent and divalent cations adsorption at mica-aqueous interface. Sci Rep, **8**(1): 12198. doi:10.1038/s41598-018-30549-9.

Anson, R.W.W., and Hawkins, A.B. 1998. The effect of calcium ions in pore water on the residual shear strength of kaolinite and sodium montmorillonite. Géotechnique, **48**(6): 787-800.

Asay, D.B., and Kim, S.H. 2005. Evolution of the adsorbed water layer structure on silicon oxide at room temperature. J. Phys. Chem. B, **109**: 16760-16763.

Atkins, P., and de Paula, J. 2006. Physical chemistry. Oxford University Press, New York.

Barbour, S.L., and Fredlund, D.G. 1989. Mechanisms of osmotic flow and volume change in clay soils. Canadian Geotechnical Journal, **26**(4): 551-562. doi:10.1139/t89-068.

Barbour, S.L., and Yang, N. 1993. A review of the influence of clay-brine interactions on the geotechnical properties of Ca-montmorillonitic clayey soils from western Canada. Canadian Geotechnical Journal, **30**: 920-934.

Beek, H.J., Bolt, G.H., and Bruggenwert, M.G.M. 1978. Soil chemistry. A. Basic elements. Elsevier.

Bouazza, A., Jefferis, S., and Vangpaisal, T. 2007. Investigation of the effects and degree of calcium exchange on the Atterberg limits and swelling of geosynthetic clay liners when subjected to wet–dry cycles. Geotextiles and Geomembranes, **25**(3): 170-185. doi:10.1016/j.geotexmem.2006.11.001.

Calvello, M., Lasco, M., Vassallo, R., and Di Maio, C. 2005. Compressibility and residual shear strength of smectitic clays influence of pore aqueous solutions and organic solvents. Rivista Italiana di Geotecnica, **1**: 34-36.

Cantrell, W., and Ewing, E. 2001. Thin Film Water on Muscovite Mica. J. Phys. Chem. B,(105): 5434-5439.

Cardoso, R., Romero, E., Lima, A., and Ferrari, A. 2007. A comparative study of soil suction measurement using two different high-range psychrometers. *In* Experimental Unsaturated Soil Mechanics. Springer-Verlag, Berlin. pp. 79-93.

Castellan, G.W. 1983. Physical chemistry. 3rd ed. Addison-Wesley Publishing Company.

Chen, L., He, X., Liu, H., Qian, L., and Kim, S.H. 2018. Water Adsorption on Hydrophilic and Hydrophobic Surfaces of Silicon. The Journal of Physical Chemistry C, **122**(21): 11385-11391. doi:10.1021/acs.jpcc.8b01821.

Chen, Y.-G., Jia, L.-Y., Li, Q., Ye, W.-M., Cui, Y.-J., and Chen, B. 2017. Swelling deformation of compacted GMZ bentonite experiencing chemical cycles of sodium-calcium exchange and salinization-desalinization effect. Applied Clay Science, **141**: 55-63. doi:10.1016/j.clay.2017.02.016.

Cheng, L., Fenter, P., Nagy, K.L., Schlegel, M.L., and Sturchio, N.C. 2001. Molecular-scale density oscillations in water adjacent to a mica surface. Phys Rev Lett, **87**(15): 156103. doi:10.1103/PhysRevLett.87.156103.

Citrini, D., and Noseda, G. 1987. Idraulica.

Decagon. 2010. WP4C Dewpoint Potentiameter - Operator's Manual - - Decagon Devices.

Di Maio, C. 1996. Exposure of bentonite to salt solution: osmotic and mechanical effects. Géotechnique, **46**(4): 695-707. doi:10.1680/geot.1996.46.4.695.

Di Maio, C. 2004. Shear strength of clays and clayey soils: the influence of pore fluid composition. *In* Chemo-Mechanical Couplings in Porous Media Geomechanics and Biomechanics. *Edited by* B. Loret and J.M. Huyghe. Springer, Berlin. pp. 45-55.

Di Maio, C., and Fenelli, G.B. 1994. Residual strength of kaolin and bentonite: the influence of their constituent pore fluid. Géotechnique, **44**(4): 217-226.

Di Maio, C., and Fenelli, G.B. 1997. Influenza delle interazioni chimico-fisiche sulla deformabilità di alcuni terreni argillosi. Rivista Italiana di Geotecnica, **1**: 43-60.

Di Maio, C., and Scaringi, G. 2016. Shear displacements induced by decrease in pore solution concentration on a pre-existing slip surface. Engineering Geology, **200**: 1-9. doi:10.1016/j.enggeo.2015.11.007.

Di Maio, C., Santoli, L., and Schiavone, P. 2004. Volume change behaviour of clays: the influence of mineral composition, pore fluid composition and stress state. Mechanics of Materials, **36**: 435-451. doi:10.1016/s0167-6636(03)00070-x.

Di Maio, C., Scaringi, G., Vassallo, R., Rizzo, E., and Perrone, A. 2016. Pore fluid composition in a clayey landslide of marine origin and its influence on shear strength along the slip surface. *In* Landslides and Engineered Slopes. Experience, Theory and Practice. pp. 813-820.

Dominijanni, A., and Manassero, M. 2012a. Modelling the swelling and osmotic properties of clay soils. Part II: The physical approach. International Journal of Engineering Science, **51**: 51-73. doi:10.1016/j.ijengsci.2011.11.001.

Dominijanni, A., and Manassero, M. 2012b. Modelling the swelling and osmotic properties of clay soils. Part I: The phenomenological approach. International Journal of Engineering Science, **51**: 32-50. doi:10.1016/j.ijengsci.2011.11.003.

Dominijanni, A., Manassero, M., and Puma, S. 2013. Coupled chemical-hydraulic-mechanical behaviour of bentonites. Géotechnique, **63**(3): 191-205. doi:10.1680/geot.SIP13.P.010.

Dutta, J., and Mishra, A.K. 2016. Consolidation behaviour of bentonites in the presence of salt solutions. Applied Clay Science, **120**: 61-69. doi:10.1016/j.clay.2015.12.001.

Ferrari, A., Favero, V., Marschall, P., and Laloui, L. 2014. Experimental analysis of the water retention behaviour of shales. International Journal of Rock Mechanics and Mining Sciences, **72**: 61-70. doi:10.1016/j.ijrmms.2014.08.011.

Fredlund, D.G., and Rahardjo, H. 1993. Soil mechanics for unsaturated soils. John Wiley and Sons, New York.

Goncalves, J., Rousseau-Gueutin, P., and Revil, A. 2007. Introducing interacting diffuse layers in TLM calculations: a reappraisal of the influence of the pore size on the swelling pressure and the osmotic efficiency of compacted bentonites. J Colloid Interface Sci, **316**(1): 92-99.

doi:10.1016/j.jcis.2007.07.023.
Hueckel, T. 1992. On effective stress concepts and deformation in clays subjected to environmental loads: Discussion. Canadian Geotechnical Journal, **29**: 1120-1125.
Jougnot, D., Revil, A., and Leroy, P. 2009. Diffusion of ionic tracers in the Callovo-Oxfordian clay-rock using the Donnan equilibrium model and the formation factor. Geochimica et Cosmochimica Acta, **73**(10): 2712-2726. doi:10.1016/j.gca.2009.01.035.
Kenney, T.C. 1967. The influence of mineral composition on the residual strength of natural soils. *In* Proc. Geotech. Conf. Shear Properties of Natural Soils and Rocks. pp. 123-129.
Lambe, T.W., and Whitman. 1969. Soil Mechanics. Wiley.
Lambe, T.W. 1960. A mechanistic picture of shear strength in clay. *In* ASCE Conference on Shear Strength of Cohesive Soils. Boulder, Colo. pp. 503-532.
Lang, A.R.G. 1967. Osmotic coefficients and water potentials of sodium chloride solutions from 0 to 40 °C. Australian J. Chem., **20**: 2017-2023.
Leroy, P., and Revil, A. 2009. A mechanistic model for the spectral induced polarization of clay materials. Journal of Geophysical Research, **114**(B10). doi:10.1029/2008jb006114.
Leroy, P., Revil, A., Altmann, S., and Tournassat, C. 2007. Modeling the composition of the pore water in a clay-rock geological formation (Callovo-Oxfordian, France). Geochimica et Cosmochimica Acta, **71**(5): 1087-1097. doi:10.1016/j.gca.2006.11.009.
Manca, D., Ferrari, A., and Laloui, L. 2016. Fabric evolution and the related swelling behaviour of a sand/bentonite mixture upon hydro-chemo-mechanical loadings. Géotechnique, **66**(1): 41-57. doi:10.1680/jgeot.15.P.073.
Mante, P.A., Chen, C.C., Wen, Y.C., Chen, H.Y., Yang, S.C., Huang, Y.R., Chen, I.J., Chen, Y.W., Gusev, V., Chen, M.J., Kuo, J.L., Sheu, J.K., and Sun, C.K. 2014. Probing hydrophilic interface of solid/liquid-water by nanoultrasonics. Sci Rep, **4**: 6249. doi:10.1038/srep06249.
Mašín, D., and Khalili, N. 2016. Swelling phenomena and effective stress in compacted expansive clays. Canadian Geotechnical Journal, **53**(1): 134-147. doi:10.1139/cgj-2014-0479.
Mitchell, J.K., and Soga, K. 2005. Fundamentals of soil behavior. 3rd ed. Wiley, Hoboken.
Mokni, N., Romero, E., and Olivella, S. 2014. Chemo-hydro-mechanical behaviour of compacted Boom Clay: joint effects of osmotic and matric suctions. Géotechnique, **64**(9): 681-693. doi:10.1680/geot.13.P.130.
Odelius, M., Bernasconi, M., and Parrinello, M. 1997. Two Dimensional Ice Adsorbed on Mica Surface. Physical Review Letters, **78**(14): 2855-2858.
Park, S.-H., and Sposito, G. 2002. Structure of Water Adsorbed on a Mica Surface. Physical Review Letters, **89**(8). doi:10.1103/PhysRevLett.89.085501.
Revil, A., Skold, M., Hubbard, S.S., Wu, Y., Watson, D.B., and Karaoulis, M. 2013. Petrophysical properties of saprolites from the Oak Ridge Integrated Field Research Challenge site, Tennessee. Geophysics, **78**(1): D21-D40. doi:10.1190/geo2012-0176.1.

Romero, E. 1999. Characterisation and thermo-hydro-mechanical behaviour of unsaturated Boom clay: an experimental study. Universitat Politecnica de Catalunya, Spain.

Saada, A., Siffert, B., and Papirer, E. 1995. Comparison of the hydrophilicity/hydrophobicity of illites and kaolinites. Journal of Colloid and Interface Science, **174**: 185-190.

Seiphoori, A., Laloui, L., Ferrari, A., Hassan, M., and Khushefati, W.H. 2016. Water retention and swelling behaviour of granular bentonites for application in Geosynthetic Clay Liner (GCL) systems. Soils and Foundations, **56**(3): 449-459. doi:10.1016/j.sandf.2016.04.011.

Silvestroni, P. 1968. Fondamenti di Chimica. Libreria Eredi Virgilio Veschi, Roma.

Skempton, A.W. 1953. The Colloidal "Activity" of Clays. Selected papers on soil mechanics: 106-118.

Spagnoli, G., Fernández, T., Feinendegen, M., Azzam, R., and Stanjek, H. 2011. Influence of the dielectric constant, electrolyte concentration and pH of the pore fluids on the shear strength of monomineralic clays. Rivista Italiana di Geotecnica, **3**: 11-24.

Sposito, G. 1989. The chemistry of soils. Oxford University Press, New York.

Sridharan, A., and Rao, G.V. 1973. Mechanisms controlling volume change of saturated clays and the role of the effective stress concept. Géotechnique, **23**(3): 359-382.

Terzaghi, K. 1936. The shearing resistance of saturated soils and the angle betweeen the planes of shear. *In* International Conference on Soil Mechanics and Foundation Engineering. Harvard University Press: Cambridge, MA. pp. 54-56.

Terzaghi, K., Peck, R., and Mesri, G. 1996. Soil mechanics in engineering practice.

Tournassat, C., Chapron, Y., Leroy, P., Bizi, M., and Boulahya, F. 2009. Comparison of molecular dynamics simulations with triple layer and modified Gouy-Chapman models in a 0.1M NaCl-montmorillonite system. J Colloid Interface Sci, **339**(2): 533-541. doi:10.1016/j.jcis.2009.06.051.

van Oort, E. 2003. On the physical and chemical stability of shales. Journal of Petroleum Science and Engineering, **38**(3-4): 213-235. doi:10.1016/s0920-4105(03)00034-2.

van Oss, C.J., and Giese, R.F. 1995. The hydrophilicity and hydrophobicity of clay minerals. Clays and Clay Minerals, **43**(4): 474-477.

Wei, C. 2014. A Theoretical Framework for Modeling the Chemomechanical Behavior of Unsaturated Soils. Vadose Zone Journal, **13**(9). doi:10.2136/vzj2013.07.0132.

Witteveen, P., Ferrari, A., and Laloui, L. 2013. An experimental and constitutive investigation on the chemo-mechanical behaviour of a clay. Géotechnique, **63**(3): 244-255. doi:10.1680/geot.SIP13.P.027.

Xu, Y., Xiang, G., Jiang, H., Chen, T., and Chu, F. 2014. Role of osmotic suction in volume change of clays in salt solution. Applied Clay Science, **101**: 354-361. doi:10.1016/j.clay.2014.09.006.

Ye, W.-M., Zhang, F., Chen, Y.-G., Chen, B., and Cui, Y.-J. 2017. Influences of salt solutions and salinization-desalinization processes on the volume change of

compacted GMZ01 bentonite. Engineering Geology, **222**: 140-145. doi:10.1016/j.enggeo.2017.04.002.

Yukselen-Aksoy, Y., Kaya, A., and Ören, A.H. 2008. Seawater effect on consistency limits and compressibility characteristics of clays. Engineering Geology, **102**(1-2): 54-61. doi:10.1016/j.enggeo.2008.07.005.

Zhao, G., Tan, Q., Xiang, L., Cai, D., Zeng, H., Yi, H., Ni, Z., and Chen, Y. 2015. Structure and properties of water film adsorbed on mica surfaces. J Chem Phys, **143**(10): 104705. doi:10.1063/1.4930274.

List of symbols

a_w	Water activity of bulk water and of the water within the system adopted for measuring or controlling the water pressure
a_{pw}	Pore water activity
c	Concentration
c'	Cohesion
c_0	Density of charge in the bulk water and in the system adopted for measuring or controlling the water pressure
$c_{fix,e}$	Effective density of fixed charge
c_{fix}	Density of fixed charge
CEC	Cation Exchange Capacity
CEC_m	Cation Exchange Capacity of the pure mineral m
C^e_{ijkl}	Drained elastic compliance tensor
e	Void ratio
G_s	Specific gravity
I_a	Activity index
M_{pw}	Molar mass of the pore water
M_w	Molar mass of the bulk water and of the water within the system adopted for measuring or controlling the water pressure
n	Porosity
R	Gas constant
R^2	Coefficient of determination
S_r	Degree of saturation
s_s	Solute suction of the bulk water and of the water within the system adopted for measuring or controlling the water pressure
$s_{s,pw}$	Solute suction of the pore water
$s_{s,e}$	Effective solute suction
T	Temperature
u^0	Reference pressure
u_w	Water pressure measured or imposed externally
u_{pw}	Pore water pressure

u_v^0	Vapor pressure of the pure liquid
$u_{v,pw}$	Vapor pressure above the pore water
$u_{v,w}$	Vapor pressure above the bulk water and above the water of the system adopted for measuring or controlling the water pressure
$\overline{V}_w^0$	Molar volume of the pure water
w_l	Liquid limit
$w_{l,DW}$	Liquid limit determined with distilled water
w_p	Plastic limit
$w_{p,DW}$	Plastic limit determined with distilled water
$x_{+,pw}$,$x_{-,pw}$	Mole fractions of positive and negative ions in the pore water
x_+,x_-	Mole fractions of positive and negative ions in the bulk water and in the water of the system adopted for measuring or controlling the water pressure
x_{pw}	Mole fraction of the pore water
x_w	Mole fraction of the bulk water
y_m	Fraction of the clay mineral m
γ_+, γ_-	Activity coefficients of positive and negative ions
δ	Reduction factor
δ_{ij}	Kronecker delta
$\dot{\varepsilon}_{ij}^e$	Rate of elastic strain of the soil skeleton
$\mu_{w,1}$,$\mu_{w,2}$	Chemical potential of the water at points 1 and 2
μ_w^0	Chemical potential of the pure water
$\nu_{+,pw}$,$\nu_{-,pw}$	Valence numbers of a species with positive or negative oxidation number in the pore water
ν_+,ν_-	Valence numbers of a species with positive or negative oxidation number in the bulk water and in the system adopted for measuring or controlling the water pressure
ρ_d	Dry density
ρ_{pw}	Pore water density
ρ_s	Solid particles density
ρ_w	Bulk water density and density of the water in the system adopted for measuring or controlling the water pressure
σ_{ij}	Total stress tensor
σ'_{ij}	Effective stress tensor
σ'_a	Axial effective stress
$\dot{\sigma}'_{kl}$	Effective stress tensor increment
σ_n	Normal total stress
$\sigma'_{n,Terzaghi}$	Terzaghi's normal effective stress
τ_f	Shear strength
φ'	Shear strength angle

Tables

Table I.
Mineralogical information of Ponza bentonite and CEC_m reference values.

Clay Mineral, m	Mineral fraction, y_m[-]	Cation Exchange Capacity of pure clay mineral, CEC_m [cmol/kg]
Kaolinite	0.20*	8.50†
Illite	0.00*	20.00†
Montmorillonite	0.80*	90.00†

* Di Maio et al. (2004)
† Mitchell and Soga (2005)

Table II.
Summary table for the interpretation of the shear strength envelope provided in Fig. 3b.

Liquid solution	$\sigma'_{n,Terzaghi}$ [kPa]	e [-]	$s_{s,e}$[kPa]	σ'_n [kPa]	τ_f [kPa]
DW	69	5.36	139	-70*	13
	86	5.03	148	-62*	14
	104	4.75	157	-53*	15
	156	4.15	180	-24*	20
	204	3.74	199	5	22
	255	3.41	219	36	29
	302	3.16	236	66	34
	399	2.75	272	127	45
0.2 M NaCl	56	2.88	39	17	16
	84	2.76	42	41	22
	106	2.68	45	61	26
	159	2.56	49	110	35
	203	2.49	52	151	41
	257	2.42	55	202	49
	300	2.37	57	243	56
	355	2.32	59	295	66
	416	2.28	61	354	80
0.5 M NaCl	44	2.06	31	13	17
	84	1.97	34	50	27
	134	1.91	36	99	36
	157	1.89	36	121	45
	207	1.85	38	169	53
	255	1.82	39	216	65
	305	1.80	40	265	78
	354	1.78	41	313	91
	415	1.76	42	373	105
1 M NaCl	55	1.47	30	26	18
	77	1.45	31	46	23
	121	1.41	32	89	36
	173	1.39	33	140	48
	220	1.37	34	185	59
	270	1.36	35	235	70
	318	1.35	35	282	83
	356	1.34	36	320	96
	413	1.33	36	376	111

6.1 M NaCl	105	0.99	11	94	36
	199	0.97	12	187	63
	299	0.95	12	287	84
	400	0.94	12	387	107

*the negative values of the effective stress correspond to non-zero values of the shear strength of the active clay; such values are to be attributed to a real cohesion (cfr. Lambe and Whitman (1969)).

Table III.
Summary table of δ reduction parameters back-predicted or estimated in this study.

Geomaterial	δ [-]
Ponza bentonite (shear strength analysis - experimental data from Di Maio (1996))	0.15*
Ponza bentonite (volumetric analysis - experimental data from Di Maio et al. (2004))	0.15*
Gela clay (volumetric analysis - experimental data from Di Maio and Fenelli (1997))	0.11†
Illite (volumetric analysis - experimental data from Spagnoli et al. (2011))	0.09†

*Back-predicted
†Estimated

Figure captions

Fig. 1. Water and ions definitions in active clays.

Fig. 2. Theoretical physical model adopted for the determination of the pore water pressure of a saturated active clay (size of the solid components is not at the scale).

Fig. 3. Shear strength envelopes for various concentrations of NaCl according to the (a) Terzaghi's effective stress. (b) generalized effective stress. Linear regression models are provided in the figure. Experimental data reported by Di Maio (1996).

Fig. 4. Solute suction of NaCl solutions having various NaCl concentrations. The proposed polynomial function is provided in the figure, together with the values of interest. Experimental data from Witteveen et al. (2013) and (Lang 1967).

Fig. 5. Elastic cycles associated with pore water chemical changes. Experimental data reported by Di Maio (1996) (Ponza bentonite) and Di Maio and Fenelli (1997) (Gela clay).

Fig. 6. Oedometer curves of Ponza bentonite subjected to chemo-mechanical paths according to two different interpretations ("NaCl" stands for 6.1 M NaCl solution): (left) Terzaghi's effective stress; (right) generalized effective stress. Experimental data reported by Di Maio (1996).

Fig. 7. (a) Effective solute suction for different NaCl concentrations; (b) liquid limit for various salt concentrations. Experimental data from Di Maio (1996) and Spagnoli et al. (2011).

Appendix A. Solute suction of the water in System B and P as a function of the differential pressure gauge reading

A thermodynamic approach is adopted. In particular, the principle of thermodynamic equilibrium relative to a generic constituent of a mixture (Atkins and de Paula 2006; Castellan 1983) is applied to the water at two different points of System C and System B of Fig. 2, respectively. Such points are considered to be at the same elevation of points 1 and 2 in Fig. 2 and are named 3 and 4 in the present discussion.
Considering the general expression of the chemical potential for an uncharged constituent of a real liquid mixture (according to the rational system of activities, Castellan 1983), the chemical potential of water at points 3 and 4, at temperature T and reference pressure u^0, can be written as follows:

$$\begin{aligned}\mu_{w,3}[T,u_{w,3},a_{w,3}] &= \mu_w^0[T,u^0]+\overline{V_w^0}(u_{w,3}-u^0)+RT\ln a_{w,3},\\ \mu_{w,4}[T,u_{w,4},a_{w,4}] &= \mu_w^0[T,u^0]+\overline{V_w^0}(u_{w,4}-u^0)+RT\ln a_{w,4},\end{aligned} \tag{A1}$$

where μ_w^0 is the chemical potentials of the pure water; $\overline{V}_w^0$ is the molar volume of the pure water; R is the gas constant; $u_{w,3}$ and $u_{w,4}$ are water pressure at points 3 and 4, respectively; $a_{w,3}$ and $a_{w,4}$ are water activity at points 3 and 4, respectively. Imposing the equality of the chemical potentials (eq. (A1)) gives

$$u_{w,3}-u_{w,4}=\frac{RT}{\overline{V_w^0}}\ln\frac{a_{w,4}}{a_{w,3}}. \tag{A2}$$

Considering that System C is characterized by pure water, $a_{w,3}=1$. Therefore

$$u_{w,3}-u_{w,4}=\frac{RT}{\overline{V_w^0}}\ln a_{w,4}. \tag{A3}$$

Since the liquid solution in System P is the same as the liquid solution in System B (the same membrane is placed between System A and the two Systems B and P) and the activity of water is independent of the point under consideration (since related to the vapor pressure), one obtains

$$u_{w,3}-u_{w,4}=\frac{RT}{\overline{V_w^0}}\ln a_w=-s_s. \tag{A4}$$

Following the procedure typically used in the presence of a differential pressure gauge (Citrini and Noseda 1987), the difference in level between the piezometric surfaces of System B and System C can be expressed as

$$\ell = h_B \frac{\gamma_{w0} - \gamma_w}{\gamma_{w0}} + \Delta \frac{\gamma_m - \gamma_{w0}}{\gamma_{w0}}, \quad \text{(A5)}$$

where Δ is the distance between the two levels reached by the manometric fluid in System M; h_B is the depth of the lowest meniscus of the differential manometer with respect to the piezometric surface of the liquid within System B; γ_m is the unit weight of the piezometric fluid (higher than those of the solutions under examination); γ_w is the unit weight of the water in System B; and γ_{w0} is the unit weight of the water in System C. By calculating the pressure of the water as the product between the unit weight and the depth of the considered point with respect to the corresponding piezometric surface (positive sign if the point is below the piezometric surface) making explicit the distance ℓ between the piezometric surfaces of the liquids in B and C (eq. (A5)), and exploiting the information that water pressure at point 4 is the one measured by piezometer P (i.e., u_w), the difference of pressure between points 3 and 4 can be written as:

$$u_{w,3} - u_{w,4} = -\frac{\gamma_w - \gamma_{w0}}{\gamma_w} u_w - h_B(\gamma_{w0} - \gamma_w) - \Delta(\gamma_m - \gamma_{w0}) \quad \text{(A6)}$$

with $u_w > 0$.

Therefore, considering equations (A4) and (A6), the relationship between the differential pressure gauge reading and solute suction is:

$$s_s = u_{w,4} - u_{w,3} = \frac{\gamma_w - \gamma_{w0}}{\gamma_w} u_w + h_B(\gamma_{w0} - \gamma_w) + \Delta(\gamma_m - \gamma_{w0}) \quad \text{(A7)}$$

with $s_s > 0$.

Appendix B. Relationship between the mole fractions of the solute ions in the pore water and in System P

The general expression of the electrochemical potential for a charged constituent (positive or negative) of a real liquid mixture (Atkins and de Paula 2006; Castellan 1983) at temperature T and reference pressure u^0, is:

(B1) $$\mu_{+/-}[T,u_w,x_{+/-},\gamma_{+/-},\phi]=\mu^0_{+/-}+\bar{V}^0_{+/-}(u_w-u^0)+RT\ln\gamma_{+/-}+RT\ln x_{+/-}+z_{+/-}F\phi,$$

where $\mu^0_{+/-}$ is the standard chemical potential of the solute ion; $\bar{V}^0_{+/-}$ is the molar volume of the solute ion at standard conditions; $\gamma_{+/-}$ and $x_{+/-}$ are activity coefficient (accounting for the deviation from the ideal condition) and mole fraction of the solute ions, respectively; $z_{+/-}$is the charge of the species (with sign); F is charge per mole of electrons, and ϕ is electric potential.

The electrochemical potentials of the positive and negative ions at points 1 and 2 (Fig. 2) are:

(B2)
$$\begin{aligned}
&\mu_{+,1}[T,u_{w,1},x_{+,1},\gamma_{+,1},\phi_1]=\mu^0_{+}+\bar{V}^0_{+}(u_{w,1}-u^0)+RT\ln\gamma_{+,1}+RT\ln x_{+,1}+z_{+}F\phi_1,\\
&\mu_{+,2}[T,u_{w,2},x_{+,2},\gamma_{+,2}]=\mu^0_{+}+\bar{V}^0_{+}(u_{w,2}-u^0)+RT\ln\gamma_{+,2}+RT\ln x_{+,2},\\
&\mu_{-,1}[T,u_{w,1},x_{-,1},\gamma_{-,1},\phi_1]=\mu^0_{-}+\bar{V}^0_{-}(u_{w,1}-u^0)+RT\ln\gamma_{-,1}+RT\ln x_{-,1}+z_{-}F\phi_1,\\
&\mu_{-,2}[T,u_{w,2},x_{-,2},\gamma_{-,2}]=\mu^0_{-}+\bar{V}^0_{-}(u_{w,2}-u^0)+RT\ln\gamma_{-,2}+RT\ln x_{-,2}.
\end{aligned}$$

by assuming as zero of the electric potential the one existing in System P.

According to the principle of thermodynamic equilibrium, the electrochemical potential of each ion (positive or negative) at point 1 must be equal to the electrochemical potential of the corresponding ion at point 2. Therefore

(B3)
$$\begin{aligned}
&\mu_{+,1}[T,u_{w,1},x_{+,1},\gamma_{+,1},\phi_1]=\mu_{+,2}[T,u_{w,2},x_{+,2},\gamma_{+,2}],\\
&\mu_{-,1}[T,u_{w,1},x_{-,1},\gamma_{-,1},\phi_1]=\mu_{-,2}[T,u_{w,2},x_{-,2},\gamma_{-,2}].
\end{aligned}$$

Replacing eq. (B2) in eq. (B3), yields

(B4)

$$\mu^0_{+}+\bar{V}^0_{+}(u_{w,1}-u^0)+RT\ln\gamma_{+,1}+RT\ln x_{+,1}+z_{+}F\phi_1=\mu^0_{+}+\bar{V}^0_{+}(u_{w,2}-u^0)+RT\ln\gamma_{+,2}+RT\ln x_{+,2},$$
$$\mu^0_{-}+\bar{V}^0_{-}(u_{w,1}-u^0)+RT\ln\gamma_{-,1}+RT\ln x_{-,1}+z_{-}F\phi_1=\mu^0_{-}+\bar{V}^0_{-}(u_{w,2}-u^0)+RT\ln\gamma_{-,2}+RT\ln x_{-,2}.$$

Limiting the development to the case in which the positive and negative solute ions have the same activity coefficients in the two systems (equal to or different from 0), eq. (B4) becomes

$$\begin{aligned}\bar{V}_+^0(u_{w,1}-u^0)+RT\ln x_{+,1}+z_+F\phi_1&=\bar{V}_+^0(u_{w,2}-u^0)+RT\ln x_{+,2},\\ \bar{V}_-^0(u_{w,1}-u^0)+RT\ln x_{-,1}+z_-F\phi_1&=\bar{V}_-^0(u_{w,2}-u^0)+RT\ln x_{-,2}.\end{aligned} \tag{B5}$$

Adding the two relations in eq. (B5) yields:

$$\bar{V}_+^0(u_{w,1}-u^0)+RT\ln x_{+,1}+z_+F\phi_1+z_-F\phi_1+\bar{V}_-^0(u_{w,1}-u^0)+RT\ln x_{-,1}=\bar{V}_+^0(u_{w,2}-u^0)+RT\ln x_{+,2}+\bar{V}_-^0(u_{w,2}-u^0)+RT\ln x_{-,2}. \tag{B6}$$

If the positive and the negative ions have the same valence (for instance, $z_+ = 1$ and $z_- = -1$), eq. (B6) becomes:

$$\bar{V}_+^0(u_{w,1}-u^0)+RT\ln x_{+,1}x_{-,1}+\bar{V}_-^0(u_{w,1}-u^0)=\bar{V}_+^0(u_{w,2}-u^0)+RT\ln(x_{+,2}x_{-,2})+\bar{V}_-^0(u_{w,2}-u^0). \tag{B7}$$

After some algebra, eq. (B7) becomes:

$$\left(u_{w,1}-u_{w,2}\right)\left(\bar{V}_+^0+\bar{V}_-^0\right)+RT\ln\left(x_{+,1}x_{-,1}\right)=RT\ln\left(x_{+,2}x_{-,2}\right). \tag{B8}$$

Replacing eq. (2) in eq. (B8) yields:

$$\left(\bar{V}_+^0+\bar{V}_-^0\right)\frac{RT}{\bar{V}_w^0}\ln\frac{a_{w,2}}{a_{w,1}}+RT\ln\left(x_{+,1}x_{-,1}\right)=RT\ln\left(x_{+,2}x_{-,2}\right). \tag{B9}$$

In the case of ideal liquids, eq. (B9) becomes:

$$\left(\bar{V}_+^0+\bar{V}_-^0\right)\frac{RT}{\bar{V}_w^0}\ln\frac{x_{w,2}}{x_{w,1}}+RT\ln\left(x_{+,1}x_{-,1}\right)=RT\ln\left(x_{+,2}x_{-,2}\right). \tag{B10}$$

Under the above-mentioned hypothesis, the term $(\bar{V}_+^0+\bar{V}_-^0)\frac{RT}{\bar{V}_w^0}\ln\frac{x_{w,2}}{x_{w,1}}$ can be considered negligible with respect to the other two appearing in eq. (B10). In fact, $x_{w,2}\to 1$, $x_{w,1}\to 1$, $\frac{RT}{\bar{V}_w^0}\ln\frac{x_{w,2}}{x_{w,1}}\to 0$. Similar reasoning is also provided in Wei (2014). Therefore

(B11) $$x_{+,1}x_{-,1} = x_{+,2}x_{-,2}.$$

Appendix list of symbols

a_w	Water activity
F	Charge per mole of electrons
h_B	Depth of the lowest meniscus of the differential manometer with respect to the piezometric surface of the liquid within System B
ℓ	Distance between the piezometric surfaces of the liquids in System B and System C
R	Gas constant
s_s	Solute suction of the bulk water and of the water within the system adopted for measuring or controlling the water pressure
T	Temperature
u^0	Reference pressure
u_w	Water pressure
$\overline{V}_w^0$	Molar volume of the pure water
$\bar{V}_{+/-}^0$	Molar volume of the solute ion at standard conditions
x_+, x_-	Mole fractions of positive and negative ions in the bulk water and in the water of the system adopted for measuring or controlling the water pressure
$z_{+/-}$	Charge of the species
γ_m	Unit weight of the piezometric fluid
γ_w	Unit weight of the water in System B
γ_{w0}	Unit weight of the water in System C
$\gamma_{+/-}$	Activity coefficient of the solute ion
Δ	distance between the two levels reached by the manometric fluid in System M
$\mu_{w,3}, \mu_{w,4}$	Chemical potential of the water at points 3 and 4 defined in the text
μ_w^0	Chemical potential of the pure water
$\mu_{+/-}^0$	Standard chemical potential of the solute ion
ϕ	Electric potential

Appendix reference list

Atkins, P., and de Paula, J. 2006. Physical chemistry. Oxford University Press, New York.

Castellan, G.W. 1983. Physical chemistry. 3rd ed. Addison-Wesley Publishing Company.

Citrini, D., and Noseda, G. 1987. Idraulica.

Wei, C. 2014. A Theoretical Framework for Modeling the Chemomechanical Behavior of Unsaturated Soils. Vadose Zone Journal, 13(9). doi:10.2136/vzj2013.07.0132.